



Fractal analysis of polyferric chloride-humic acid (PFC-HA) flocs in different topological spaces

WANG Yili^{1,*}, LU Jia¹, DU Baiyu¹, SHI Baoyou², WANG Dongsheng²

1. College of Environmental Science and Engineering, The Key Laboratory for Silviculture and Conservation of Ministry of Education, Beijing Forestry University, Beijing 100083, China. E-mail: wangyilimail@126.com

2. State Key Laboratory of Environmental Aquatic Chemistry, Research Center for Eco-Environmental Sciences, Chinese Academy of Sciences, Beijing 100085, China

Abstract

The fractal dimensions in different topological spaces of polyferric chloride-humic acid (PFC-HA) flocs, formed in flocculating different kinds of humic acids (HA) water at different initial pH (9.0, 7.0, 5.0) and PFC dosages, were calculated by effective density-maximum diameter, image analysis, and N₂ absorption-desorption methods, respectively. The mass fractal dimensions (D_f) of PFC-HA flocs were calculated by bi-logarithm relation of effective density with maximum diameter and Logan empirical equation. The D_f value was more than 2.0 at initial pH of 7.0, which was 11% and 13% higher than those at pH 9.0 and 5.0, respectively, indicating the most compact flocs formed in flocculated HA water at initial pH of 7.0. The image analysis for those flocs indicates that after flocculating the HA water at initial pH greater than 7.0 with PFC flocculant, the fractal dimensions of D_2 ($\log A$ vs. $\log d_L$) and D_3 ($\log V_{\text{sphere}}$ vs. $\log d_L$) of PFC-HA flocs decreased with the increase of PFC dosages, and PFC-HA flocs showed a gradually looser structure. At the optimum dosage of PFC, the D_2 ($\log A$ vs. $\log d_L$) values of the flocs show 14%–43% difference with their corresponding D_f , and they even had different tendency with the change of initial pH values. However, the D_2 values of the flocs formed at three different initial pH in HA solution had a same tendency with the corresponding D_f . Based on fractal Frenkel-Halsey-Hill (FHH) adsorption and desorption equations, the pore surface fractal dimensions (D_s) for dried powders of PFC-HA flocs formed in HA water with initial pH 9.0 and 7.0 were all close to 2.9421, and the D_s values of flocs formed at initial pH 5.0 were less than 2.3746. It indicated that the pore surface fractal dimensions of PFC-HA flocs dried powder mainly show the irregularity from the mesopore-size distribution and macropore-size distribution.

Key words: polyferric chloride-humic acid (PFC-HA) flocs; topological spaces; fractal dimensions; effective density; image analysis; pore surface fractal

Introduction

Humic acids (HAs) are one of the main constituents of natural organic matter (NOM) in surface waters (Edzwald, 1993; Edzwald and Tobiason, 1999; Jekel, 1986). It has been recognized that NOM is the primary precursor of many important disinfection byproducts (DBPs) formed during water chlorination. DBPs, such as trihalomethanes (THMs), haloacetic acids (HAAs), are suspected carcinogens, which pose great health risks to water consumers (Edzwald, 1993; Edzwald and Tobiason, 1999; Jekel, 1986). The United States Environmental Protection Agency has proposed that enhanced coagulation is a best available technology (BAT) for NOM removal. Extensive previous studies have paid the most attention to the reaction behavior between FeCl₃ and HAs (Edzwald, 1993; Edzwald and Tobiason, 1999; Jacangelo *et al.*, 1995). The results proved that FeCl₃ had good performance on HAs removal during enhanced coagulation process. However, a few studies focused on the HAs removal and coagulated

flocs with polyferric chloride (PFC), an inorganic polymer flocculant (IPF), which had a good performance on particle removal from natural water or wastewater. These research works show that PFC has good performance on HAs removal (Wang *et al.*, 2006a, 2006b), and the formed PFC-HAs flocs with fractal morphology have an important effect on HAs removal also.

A review of previous work shows floc fractal properties, such as mass fractal or fractal characteristics under different dimensions, could give some hints on the formation dynamics and the microstructure of flocs induced by coagulants. Generally, a mass fractal may have some influence on bulk physical structural characteristics, such as floc density, settling rates, and floc strength (Gregory, 1997; Li and Logan, 2001; Serra and Logan, 1999). A two-dimensional fractal dimension could indicate the compact or loose structure of flocs, and floc irregular boundary could have positive relation with the one-dimensional fractal characteristics (Feder, 1988; Gregory, 1997; Jiang and Logan, 1991; Li and Logan, 2001; Mandelbrot, 1982; Serra and Logan, 1999). In fact, the physical and chemical

* Corresponding author. E-mail: wangyilimail@126.com

properties of floc surface also have an important effect on the kinetic growing of flocs, and more irregular and rough surfaces will imply high collision and attachment rates between different flocs in flocculation/flotation and filtration ect. However, the surface fractal dimension as an indication on the irregularity and roughness of surfaces (Avnir *et al.*, 1983, 1985; Douglas, 1989; Fripiat *et al.*, 1986; Neimark and Unger, 1993; Pfeifer and Obert, 1989; Pfeifer *et al.*, 1989; Russ, 1994; Wang, 2006b, 2007) has rarely been reported in above coagulation process.

In this article, the fractal dimensions of polyferric chloride humic acid (PFC-HA) flocs in different topological spaces were studied.

1 Materials and methods

1.1 Humic acid solutions

Solutions of test water were prepared using dissolved HAs reagent (Tianjin Jinke Fine Chemical Institute, China) in deionized water and filtrated with a 0.45- μm membrane, then diluted with tap water of equal volume, corresponding to a mass concentration 4.79 mg/L (as dissolved organic carbon (DOC)) and 0.33 cm^{-1} for UV absorbance at 254 nm (UV_{254}) was performed. A 1 000-mL solution sample was used in the coagulation jar test. The initial pH of this solutions were kept at 9.00 ± 0.05 , 7.00 ± 0.05 , 5.00 ± 0.05 , respectively. Moreover, the turbidity of these solutions was close to 1.12 NTU (Turbidimeter 2100N, HACH, USA).

1.2 Coagulant

Polyferric chloride (Tianjin Tianshui Water Purifying Ltd., China) was used as coagulant. PFC, with basicity (OH/Al molar percentage) 15.4%, contained 10.4% (W/W) Fe_2O_3 and was diluted to 0.1761 mol/L solution with ultrapurified water for use.

1.3 Apparatus and procedures

1.3.1 Jar test

Coagulation experiments were carried out by performing a series of jar tests. A JTY variable-speed jar tester (Tangshan Dachang Chemical Ltd., China) was used with 50 mm \times 40 mm flat paddle impellers with cylindrical jars containing 1 L sample. Two speeds were used with a rapid mix at 200 r/min for 1.0 min, followed by a slow stir phase at 30 r/min for 15 min. Then, the flocs were allowed to settle for 30 min, after measurements of UV_{254} , turbidity measurements were taken. A 50-mL supernatant collected from just below the water surface was analyzed for UV_{254} using a UV-Vis spectrum meter (UV8500, Shanghai Tech-comp Ltd., China), and turbidity was measured at the same time. In addition, the pH of supernatant was measured. During this stage, UV_{254} removal was used as an indicator of NOM removal. Three kinds of flocs were produced at every optimum coagulant dosage. When initial pH was 9.0, 7.0, and 5.0, the corresponding optimum PFC dosages were 22.93, 14.20, and 14.20 mg/L (as Fe^{3+}), respectively, for HA solution.

1.3.2 Floc settling rate and fractal dimension

The experimental apparatus for the settling of flocs consists of a Pyrex glass column (Fig. 1). The column is 400 mm in height to ensure that the terminal settling velocity could be reached, and 30 mm in radius was set to neglect the wall effect on aggregate settling. During each run of the settling-coagulation experiments, a floc was introduced into the top of the column, which was filled with deionized water. After the slow mixing, flocs were withdrawn from the stirred tank. To ensure that the free water within the flocs was exactly the same in density as that in the setting column, prior to being introduced into the settling column, the flocs were transferred in series through two Petri dishes of water identical to that used for making solution placed in the column using a wide mouthed pipet. Flocs that broke up during any transfer steps were discarded.

Images of floc, while passing through the observation region in the Pyrex glass-settling column, were captured using a microscope objective (AVENIR TV Zoom Lens SR12575, 12.5 mm–75 mm F1.8, Japan) connected with a HV1302UM charge-coupled device (CCD) camera (China Daheng Group Corporation, Beijing Image Vision Technology Branch) and a computer. Image analysis software (MiVnt, China Daheng Group Corporation, Beijing Image Vision Technology Branch) was used to determine the floc settling velocity and had been calibrated using a yardstick. The image grabber was manually triggered to take a series of 20 images. The time between each frame was set at 1 s. This indicates that the distance traveled by the floc could be calculated per frame and therefore per time period, thus giving a settling velocity. The equivalent diameter of each floc was recorded with another HV1302UM charge-coupled device (CCD) camera after it settles to the bottom of this column and had been calibrated using a coin for approximately 120 aggregates for each set of coagulation conditions.

1.3.3 Floc image acquisition and processing

To obtain the floc images with high resolution, a image processing system (Fig. 2) was built, and its main components include a computer-controlled digital CCD camera (China Daheng Group Corporation, Beijing Image Vision Technology Branch), Computar Macro Zoom lens (MLM-

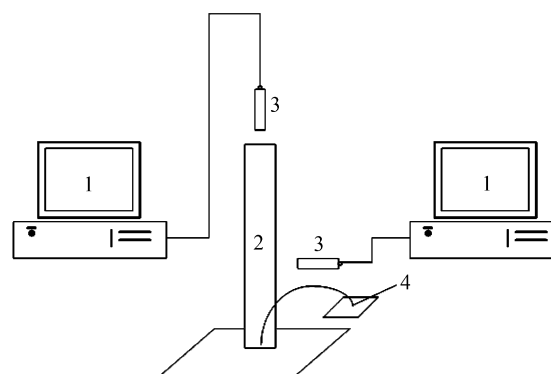


Fig. 1 Testing diagram for floc setting rate. (1) computer; (2) setting column; (3) charge-coupled device (CCD) camera; (4) flocs.

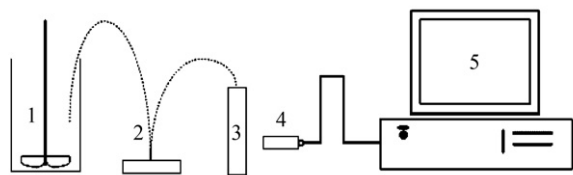


Fig. 2 Schematic methodology for floc images recording. (1) flocculation mixer; (2) petri dish; (3) colorimetric tube; (4) CCD; (5) computer.

3XMP, Goyo Optical Inc., Japan), lighting provided by a stroboscopic lamp, image acquisition, and image analysis software. The strobe light was placed on the opposite side of the jar from the camera to provide back-lighting, which produces particle images as shadows. As a focused floc was introduced into a colorimetric tube filled with deionized water and passed through the observation region in the colorimetric tube, its images were recorded by computer-controlled digital CCD camera.

1.3.4 Fractal geometry in different topological space

Geometric characteristics were derived for the images collected after slow-stirring stage at optimum dosage of coagulant. Unlike spherical particles that can be described by a single parameter of diameter only, nonspherical particles can be characterized in many ways. The software then determines the area, the perimeter, and the second-order moments of the image for each floc.

The effective density of floc can be deduced from its setting rate, and the mass fractal dimension can be calculated by regression analysis of the logarithm of the effective density versus the logarithm of the characteristic length, such as the diameter of equivalent circle and long axis of the particle image (Gregory, 1997; Wang and Tambo, 2000). When Reynolds numbers of a setting floc were between 0.1 and 1.0, the Logan empirical formula (Li and Logan, 2001; Serra and Logan, 1999) was used to calculate the fluid drag coefficient (C_D). At other large Reynolds numbers, Allen or Logan empirical formulas (Yan and Fan, 1999) could be used to estimate C_D . If C_D was determined, the effective density of a floc could be given through its relation with the setting rate.

The one-dimensional fractal dimension of flocs was calculated by regression analysis of the logarithm of their perimeter versus the logarithm of their corresponding characteristic length. The two-dimensional fractal dimension of flocs was calculated by regression analysis of the logarithm of their projected area versus the logarithm of their corresponding characteristic length or perimeter (Jin and Wang, 2001). In this work, the long diameter of the particle image was taken as the characteristic length. The three-dimensional fractal dimension of flocs cannot be calculated in a similar manner as D_2 since aggregate volume cannot be measured directly with the present apparatus. However, aggregate volume can be estimated by assuming thickness in the direction normal to the viewing direction. Thus, the equivalent spheres and ellipsoid were used to estimate floc volume. Once their volumes were calculated, D_3 could be obtained from regression analysis of these volumes versus their corresponding characteristic length similar to the procedure for D_2 (Jin and Wang, 2001). This method

of calculating D_3 essentially represents a hypothesis that information on three dimensional characteristics can be extracted from a two-dimensional image.

1.3.5 Cryofixation and vacuum drying of PFC-HA flocs

Cryofixation of PFC-HA flocs samples were carried out by plunge freezing in liquid nitrogen at 77 K. A 15-mL plastic centrifugal tube containing 10 mL flocculated water with flocs was plunged in liquid-nitrogen tank for 30 min. The cryofixation samples were put in the vacuum-freeze dryer (FD-1A, Beijing Boyikang Laboratory Instruments Ltd., China) for 24–48 h. Sublimation of the ice formed from void or interstitial water of the sample was then obtained by the vacuum-freeze drying process (Nègre *et al.*, 2004). Then, the dry floc samples were obtained and stored in a desiccator.

1.3.6 Analytical methods

The surface area and pore size distribution of the dried PFC-HA powder have been measured by nitrogen adsorption using ASAP 2000 (Micromeritics, USA).

1.3.7 Pore surface dimension

To evaluate the pore surface fractal dimension of PFC-HA, flocs have been performed using a well-established method based on the fractal version of the Frenkel-Halsey-Hill (FHH) equation and thermodynamic equation. The length scale, where fractal behavior was determined from fractal FHH equation plots, was also computed according to the references (El Shafei *et al.*, 2004; Neimark and Unger, 1993; Wang *et al.*, 2006b, 2007).

2 Results

2.1 Fractal dimensions in three-dimension topological space-mass fractal dimension

Figure 3 shows the regression plot of the logarithm of the effective density (ρ_e) of the flocs at initial pH 7.00 versus the diameter of equivalent circle (d_p) or long diameter of their images (d_L). The effective densities were given when using Logan empirical equations for fluid drag coefficient (C_D) calculation. Then, according to Eq. (1), the mass fractal dimension (D_f) can be calculated from the slope of the regression lines.

$$\rho_e \propto d_a^{D_f-3} \quad (1)$$

where, ρ_e is the effective density of floc and d_a is the diameter of equivalent circle or long diameter of floc. The regression plots for flocs at initial pH 9.0 and 5.0 had the similar shape to that at initial pH 7.0 and were omitted. The mass fractal dimensions of flocs at these three situations were given in Table 1. It is easily observed that the correlation coefficient (r) of linear regression of the logarithm of the effective density of flocs calculated by Logan empirical formulas versus long diameter of their images was higher than others. Therefore, the mass fractal dimensions can be calculated by the logarithm of the effective density of flocs calculated by Logan empirical formulas versus long diameter of their images. The mass

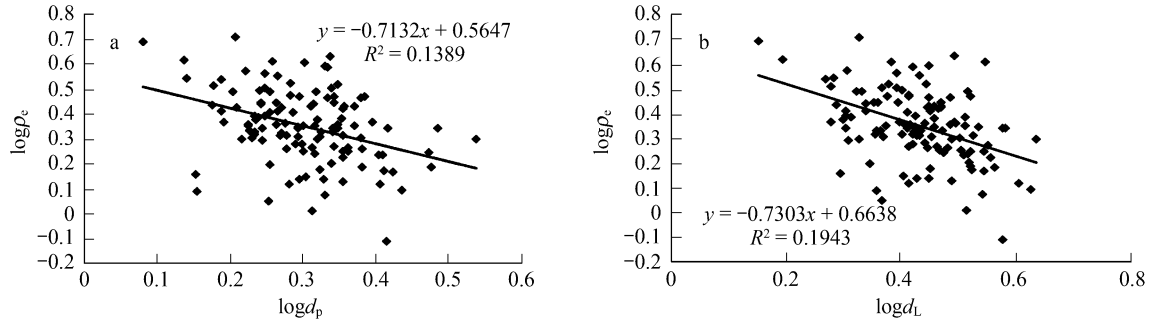


Fig. 3 $\log \rho_e$ vs. $\log d_p$ (a) and $\log \rho_e$ vs. $\log d_L$ (b) plots for polyferric chloride-humic acid (PFC-HA) flocs.

Table 1 Mass fractal dimensions (D_f) of PFC-HA flocs with numbers of about 110–120

Initial pH	$(\log \rho_e$ vs. $\log d_p$) ^a		$(\log \rho_e$ vs. $\log d_L$) ^a		$(\log \rho_e$ vs. $\log d_p$) ^b		$(\log \rho_e$ vs. $\log d_L$) ^b	
	D_f	r	D_f	r	D_f	r	D_f	r
9.00 ± 0.05	2.20	0.3359	2.23	0.415	1.87	0.5074	2.04	0.5569
7.00 ± 0.05	2.69	0.1428	2.56	0.2360	2.29	0.3727	2.27	0.4408
5.00 ± 0.05	1.70	0.6089	1.97	0.5241	1.49	0.7309	1.72	0.6679

^a Allen empirical formula; ^b Logan empirical formula.

fractal dimension of flocs at initial pH = 7.0 is higher than that at initial pH = 9.0, and the least mass fractal dimension was found for flocs at initial pH = 5.0.

2.2 Fractal dimensions based on floc images

To demonstrate the effect of coagulant dosages on the fractal dimensions of flocs, Table 2 shows that the fractal dimensions and average diameters in the different topological spaces of PFC-HA flocs formed under different PFC dosages. For HA water with initial pH 9.0, all the fractal dimensions D_1 , D_2 , D_3 in the different topological spaces of flocs continue to decrease as the PFC dosage increases. D_2 based on the logarithm of areas (A) versus long diameter ($\log A$ vs. $\log d_L$) of floc images were higher than those based on the logarithm of areas versus perimeters (P) ($\log A$ vs. $\log P$) of floc images. D_3 values were calculated by the logarithm of equivalent sphere volumes (V_{sphere}) or equivalent ellipsoid volumes ($V_{\text{ellipsoid}}$) versus long diameter of floc images. In general, equivalent ellipsoid volumes may give a more accurate estimation for volume. The average diameters fluctuated as the PFC dosage increases. For HA water with initial pH 7.0, only the fractal dimensions D_2 based on ($\log A$

vs. $\log d_L$) relation and D_3 based on ($\log V_{\text{sphere}}$ vs. $\log d_L$) relation continue to decrease as the PFC dosage increases, others fluctuate as the PFC dosage increases. For HA water with initial pH 5.0, all the fractal dimensions fluctuate as PFC dosage increases. In this work, the maximum arithmetic average diameter for flocs was about 2.31 mm in flocculated HA water at initial pH 9.0 at PFC dosage of 22.93 mg/L (as Fe^{3+}). However, the maximum arithmetic average diameter of about 2.45 mm for flocs in flocculated HA water at initial pH 7.0 at PFC dosage of 5.46 mg/L (as Fe^{3+}) and at initial pH 5.0, the maximum arithmetic average diameter was given at PFC dosage of 3.28 mg/L (as Fe^{3+}) as 1.66 mm.

2.3 Pore surface fractal dimensions

The pore surface fractal dimensions of dried PFC-HA flocs powder were calculated by fractal FHH equation or thermodynamic equation, and the corresponding linear regressions plots are shown in Fig. 4. Sample 1 was cryofixation-vacuum-freeze-dried PFC-HA flocs in flocculated HA water at initial pH 9.0, and sample 2 and sample 3 were flocs in flocculated HA water at initial pH 7.0 and 5.0, respectively. The calculated pore surface

Table 2 Fractal dimensions and average diameters in the different topological spaces of PFC-HA flocs

Initial pH	PFC (mg/L, as Fe^{3+})	Fractal dimensions in the different topological spaces					Diameter (mm)	
		D_1 ($\log P$ vs. $\log d_L$) (R^2)	D_2 ($\log A$ vs. $\log d_L$) (R^2)	D_2 ($\log A$ vs. $\log P$) (R^2)	D_3 ($\log V_{\text{sphere}}$ vs. $\log d_L$) (R^2)	D_3 ($\log V_{\text{ellipsoid}}$ vs. $\log d_L$) (R^2)	Median	Arithmetic
9.00 ± 0.05	3.28	1.17 (0.95)	1.97 (0.95)	1.66 (0.96)	2.96 (0.95)	2.99 (0.88)	1.95	1.89
	5.46	1.11 (0.93)	1.82 (0.90)	1.61 (0.93)	2.73 (0.90)	2.68 (0.83)	2.06	2.09
	10.92	1.08 (0.93)	1.78 (0.92)	1.56 (0.89)	2.67 (0.92)	2.62 (0.85)	1.87	1.90
	22.93	1.05 (0.80)	1.74 (0.76)	1.54 (0.81)	2.62 (0.76)	2.56 (0.65)	2.37	2.31
7.00 ± 0.05	3.28	1.15 (0.92)	1.89 (0.94)	1.55 (0.91)	2.83 (0.94)	2.86 (0.92)	2.20	2.16
	5.46	1.04 (0.90)	1.71 (0.88)	1.56 (0.87)	2.56 (0.88)	2.38 (0.77)	2.48	2.45
	14.20	1.13 (0.76)	1.59 (0.77)	1.22 (0.76)	2.38 (0.77)	2.25 (0.63)	2.13	2.08
	26.21	1.17 (0.93)	1.46 (0.84)	1.24 (0.90)	2.19 (0.84)	2.47 (0.77)	0.65	0.67
5.00 ± 0.05	3.28	1.09 (0.95)	1.78 (0.92)	1.60 (0.94)	2.67 (0.92)	2.72 (0.88)	1.57	1.66
	5.46	1.09 (0.99)	1.95 (0.99)	1.79 (0.99)	2.93 (0.99)	3.21 (0.97)	1.40	1.37
	14.20	1.04 (0.83)	1.50 (0.79)	1.36 (0.84)	2.25 (0.79)	2.25 (0.66)	1.29	1.29

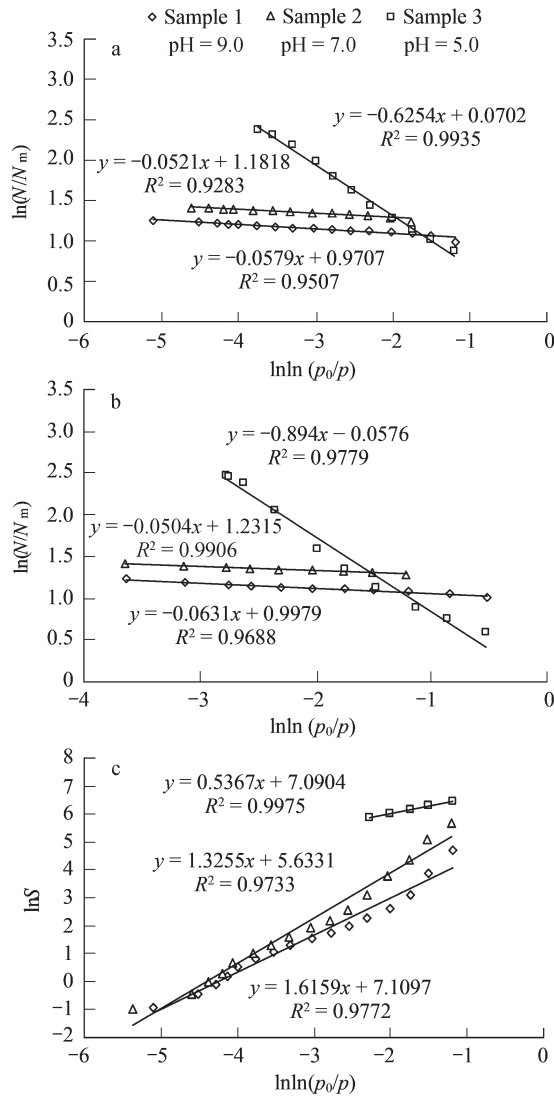


Fig. 4 Fractal analysis according to fractal FHH isotherm equation and thermodynamic model for cryofixation-vacuum-freeze-dried PFC-HA flocs powder. (a) fractal FHH adsorption; (b) fractal FHH desorption; (c) thermodynamic equation. N/N_m : fractions of surface coverage; P_0/P : ratio of saturation and equilibrium pressures of the adsorbate; S : area of the “condensed adsorbate-vapor” equilibrium interface.

fractal dimensions of dried powder are given in Table 3. For HA water with initial pH 9.0 and 7.0, the pore surface fractal dimensions at optimum PFC dosage were 2.9421 and 2.9479 respectively, based on fractal FHH equation. A little difference was shown when using the nitrogen adsorption data and desorption data. However, for HA water with initial pH 5.0, the pore surface fractal dimension for these dried powder at optimum PFC dosage

was 2.3746 based on fractal FHH equation with nitrogen adsorption data and 2.106 with nitrogen desorption data. When using thermodynamic equation, their pore surface fractal dimensions at optimum PFC dosage were different from that using fractal FHH equation and often show values higher than 3 (except at pH 5.0).

3 Discussion

In the floc settling-speed test, the geometric parameters of PFC-HA flocs at horizontal projected view and vertical projected view can be calculated using MiVnt software. The ratio between the average diameters (arithmetic average diameter or median diameter) for PFC-HA flocs at horizontal projected view and at vertical projected view were close to 0.85 (Table 4).

The settling rates and effective densities of flocs formed in different initial pH vs. equivalent diameters are shown in Fig. 5. Fig. 5a indicates that the settling rates of flocs formed in initial pH 5.0 were mostly less than the flocs with the same size formed under initial pH 7.0 and 9.0. The ratio among the average settling rates for those flocs in HA water at initial pH 9.0, 7.0, and 5.0 was 1.11:1:0.50. In Fig. 5b, except for one floc, the effective densities of other flocs formed in initial pH 5.0 were less than the flocs with the same size formed at pH 9.0 and 7.0. The ratio among the average effective density for those flocs in HA water at initial pH of 9.0, 7.0, and 5.0 was 1.11:1:0.98 for Allen empirical formula, and 1.09:1:1.42 for Logan empirical formula.

The mass fractal dimensions (D_f) of PFC-HA flocs, being more than 2.0, calculated by bi-logarithm relation of effective density-maximum diameter and Logan empirical formula at initial pH 7.0 had 11%–13% greater than those at other initial pH. Therefore, in comparison with the PFC-HA flocs in HA water at initial pH of 5.0 and 9.0, the most compact flocs were formed in HA water at initial pH of 7.0, and the very smaller and looser flocs were formed in HA

Table 4 Average diameter (arithmetic average diameter/median diameter) and their ratio of PFC-HA flocs at different projected views

Initial pH	Average $d_{p,H}$ (mm)	Average $d_{p,V}$ (mm)	Average $d_{p,H}/$ Average $d_{p,V}$
9.00 ± 0.05	1.8736/1.8486	2.1784/2.1660	0.8601/0.8535
7.00 ± 0.05	1.7115/1.6661	2.0209/1.9784	0.8469/0.8421
5.00 ± 0.05	0.9807/0.9518	1.1476/1.1295	0.8546/0.8427

Average $d_{p,H}$: average diameter for PFC-HA flocs at horizontal projected view; Average $d_{p,V}$: average diameter for PFC-HA flocs at vertical projected view.

Table 3 Pore surface fractal dimensions of cryofixation-vacuum-freeze-dried PFC-HA flocs powder

Initial pH	FHH desorption equation	FHH desorption equation	Thermodynamic equation
9.00 ± 0.05	2.9421 ($R^2 = 0.9507$) (0.7375 < x < 0.9939)	2.9369 ($R^2 = 0.9688$) (0.552 < x < 0.9738)	3.3255 ($R^2 = 0.9772$) (0.7375 < x < 0.9939)
7.00 ± 0.05	2.9479 ($R^2 = 0.9283$) (0.8423 < x < 0.99)	2.9496 ($R^2 = 0.9906$) (0.7436 < x < 0.9742)	3.6159 ($R^2 = 0.9733$) (0.7392 < x < 0.9953)
5.00 ± 0.05	2.3746 ($R^2 = 0.9935$) (0.7388 < x < 0.9765)	2.106 ($R^2 = 0.9779$) (0.5547 < x < 0.9394)	2.5367 ($R^2 = 0.9975$) (0.7388 < x < 0.9028)

R^2 : linear definite coefficient; x : ratio of p and p_0 .

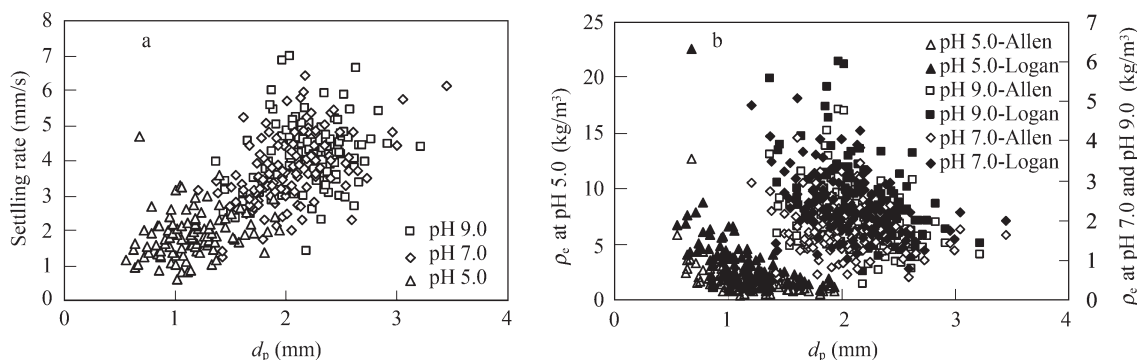


Fig. 5 Settling rate vs. equivalent diameter (a) and effective density vs. equivalent diameter (b).

water at initial pH of 5.0 and their D_f values were less than 2.0. At initial pH of 9.0, the D_f values of flocculated PFC-HA flocs were close to 2.0 (Table 1). Combining the data of setting rates and effective densities of flocs, it revealed that mass fractal dimensions, effective density, and diameter of PFC-HA flocs could affect their setting rates, and both the highest value of mass fractal dimensions or effective density of PFC-HA flocs could not express the highest settling rate totally.

As shown in Table 2, the image analysis for those flocs indicates that after flocculating the HA water at initial pH greater than 7.0 with PFC flocculant, the fractal dimensions of D_2 ($\log A$ vs. $\log d_L$) and D_3 ($\log V_{\text{sphere}}$ vs. $\log d_L$) of PFC-HA flocs decreased with the increase in PFC dosages and flocs showed a gradually looser structure. At the optimum dosage of PFC, the D_2 ($\log A$ vs. $\log d_L$) values of the flocs showed 14%–43% difference with their corresponding D_f . The D_3 ($\log V_{\text{sphere}}$ vs. $\log d_L$) or D_3 ($\log V_{\text{ellipsoid}}$ vs. $\log d_L$) values of the flocs showed 41%–50%, about 50% difference, respectively. Besides those, the D_2 ($\log A$ vs. $\log d_L$) of the flocs formed under three initial HA solution pH showed a different tendency with the corresponding D_f . These differences maybe caused by different floc images used for D_f and D_2 or D_3 calculation. The floc images for D_f calculation were recorded by CCD system in Fig. 1, and its magnification is in the range 6–9, but the flocs images for D_2 or D_3 calculation were recorded by CCD system in Fig. 2, and its magnification is in the range 26–31. The D_1 , D_2 , and D_3 values were calculated based on the floc images recorded by the CCD system in Fig. 1, and these flocs were also used in above D_f calculation. It showed that the D_2 values of the flocs formed at three different initial HA solution pH, based on the horizontal projected images with magnification of about 9, had a same tendency with the corresponding D_f .

The powder for above PFC-HA flocs were prepared by cryo-freeze-vacuum-dried method, and then were characterized by microstructure measurement. Their microstructure was investigated by N_2 absorption-desorption method. It was observed that sample 3 (initial pH 5.0) has a hysteresis loop in the N_2 absorption-desorption isotherm with a different shape from other two samples. The adsorption volume, Barret-Joyner-Halenda (BJH) cumulative absorption volume of pores, and BJH desorption average pore diameter of sample 3 were much higher than those

of other samples, and those parameters of sample 2 (initial pH 7.0) were higher than sample 1 to certain extent. The pore-size distribution (PSD) of sample 3 shows that some macropores exist in its surface. However, the BET specific surface area of these samples has a different trend from above surface geometrical parameters, and that of sample 2 was a little larger than that of sample 3, and the sample 1 (initial pH 9.0) possessed the smallest. In general, the pore surface fractal dimensions (D_s) for sample 1, sample 2, and sample 3 showed that the former two samples had more ability for space-filling than the later one.

Although the geometrical irregularities and roughness of the surface are the essential reasons for the obtained D_s , it is known that absorbed film volume and pore size distribution are used to define fractal in fractal FHH equation. The FHH type equation might be sensitive to the pore size distribution, therefore, pore size distribution can contribute significantly to the surface fractal dimension (El Shafei *et al.*, 2004; Neimark and Unger, 1993; Sokołowska and Sokołowski, 1999). If the pore size distribution is fractal, the following Eq. (2) could be used to express these fractal relations.

$$J(r) = br^{2-D_s} \quad (2)$$

where, $J(r)$ is the pore size distribution function, r is pore radius, and D_s is the surface fractal dimensions determined by pore size distribution. Therefore, the corresponding D_s for dried powder of PFC-HA flocs are listed in Table 6. Compare to the fractal dimensions for pore-size distribution, it can be shown that these pore surface fractal dimensions (Table 3) of PFC-HA flocs powder cannot totally represent the space-filling capability of irregular pore surface but mainly show the irregularity from the mesopore-size distribution and some macropore-size distribution.

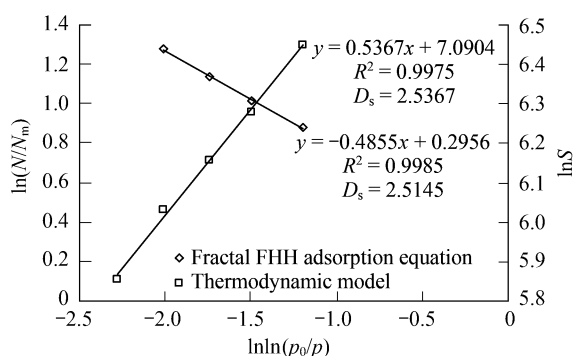
In addition, compared with the fractal FHH equation, the significant high pore surface D_s values for these samples were calculated through thermodynamic model, and most of them exceeded 3 (Table 3). Due to the hysteresis loop of a model in the N_2 absorption-desorption isotherm for sample 3 (Zhao, 2005), the close values of its pore surface fractal dimension could be determined by both thermodynamic model and fractal FHH adsorption equation if the fractal scale is reduced. This result is given in Fig. 6, the former fractal scale is in the range 3.17–7.12 nm, and the

Table 5 Fractal dimensions of PFC-HA flocs in the onedimensional (D_1) and twodimensional (D_2) topological spaces

Initial pH	Vertical projected view			Horizontal projected view		
	D_1 (logP vs. $\log d_L$)	D_2 (logA vs. $\log d_L$)	D_2 (logA vs. $\log P$)	D_1 (logP vs. $\log d_L$)	D_2 (logA vs. $\log d_L$)	D_2 (logA vs. $\log P$)
9.00 ± 0.05	1.12 ($R^2=0.8418$)	1.41 ($R^2=0.8310$)	1.09 ($R^2=0.7427$)	1.04 ($R^2=0.8122$)	1.39 ($R^2=0.6354$)	1.17 ($R^2=0.5965$)
7.00 ± 0.05	1.02 ($R^2=0.8676$)	1.52 ($R^2=0.7705$)	1.37 ($R^2=0.7457$)	1.02 ($R^2=0.8024$)	1.64 ($R^2=0.6779$)	1.37 ($R^2=0.6103$)
5.00 ± 0.05	1.07 ($R^2=0.9271$)	1.66 ($R^2=0.8195$)	1.55 ($R^2=0.8831$)	1.07 ($R^2=0.8017$)	1.33 ($R^2=0.7616$)	1.07 ($R^2=0.7255$)

Table 6 Pore surface fractal dimensions (D_s) of cryofixation-vacuum-freeze-dried PFC-HA flocs based on pore-size distribution

Initial pH	BJH adsorption pore distribution		BJH desorption pore distribution	
	D_s	Pore size (nm)	D_s	Pore size (nm)
9.00 ± 0.05	2.8839 ($R^2=0.9522$)	3.06–155.84	2.9512 ($R^2=0.9128$)	1.81–37.03
7.00 ± 0.05	2.9985 ($R^2=0.9740$)	6.52–99.07	3.1573 ($R^2=0.9332$)	3.61–37.62
5.00 ± 0.05	2.2652 ($R^2=0.8051$)	3.13–46.12	2.1179 ($R^2=0.7397$)	1.80–17.93

**Fig. 6** Fractal analysis according to fractal FHH isotherm equation and thermodynamic model for sample 3.

latter is in the range 2.15–4.84 nm (data not shown).

4 Conclusions

The PFC-HA floc effective density can be estimated by its settling-speed using Logan empirical formula and the mass fractal dimensions D_f of PFC-HA flocs, being more than 2.0, calculated by bi-logarithm relation of effective density-maximum diameter. Logan empirical formula at initial pH 7.0 had 11% or 13% greater than those at other initial pH 9.0 or 5.0, which indicated that the most compact flocs were formed in HA water at initial pH 7.0. Both the highest value of D_f or effective density of PFC-HA flocs could not express their highest settling rate completely.

The image analysis for PFC-HA flocs indicated that after flocculating the HA water at initial pH greater than 7.0 with PFC flocculant, the fractal dimensions of D_2 (logA vs. $\log d_L$) and D_3 ($\log V_{\text{sphere}}$ vs. $\log d_L$) of PFC-HA flocs decreased with the increase in PFC dosages, and PFC-HA flocs showed a gradually looser structure. However, the fractal dimensions of PFC-HA flocs in flocculated water at initial pH 5.0 fluctuated with the addition of PFC. At the optimum dosage of PFC, the D_2 (logA vs. $\log d_L$) values of the flocs show 14%–43% difference with their corresponding D_f , even had different tendency as the change of initial pH values. But the D_2 values of the flocs formed under three initial HA solution pH, calculated from the horizontal projected images with magnification of about 9, had a same tendency with the corresponding D_f ones.

The pore-size distribution (PSD) of sample 3 (initial pH 5.0) shows that some macropores exist in its surface, and BET specific surface area of these samples indicates that sample 1 (initial pH 9.0) possesses the smallest one among them. Based on fractal FHH adsorption and desorption equations, the pore surface fractal dimensions D_s for dried powders of sample 1 (initial pH 9.0) and sample 2 (initial pH 7.0) were all close to 2.9421, but D_s values of sample 3 (initial pH 5.0) were less than 2.3746. It appears that these pore surface fractal dimensions of PFC-HA flocs powder cannot fully represent the space-filling capability of irregular pore surface but mainly show the irregularity from the mesopore-size distribution and some macropore-size distribution.

Acknowledgments

This work was supported by the National Natural Science Foundation of China (No. 20407004, 50578012, 50178009), the High-Tech Research and Development Program (863) of China (No. 2007AA06Z301), the Fok Ying Tung Education Foundation of National Education Ministry of China (No. 91078), the Beijing Municipal Commission of Education Project, Program for New Century Excellent Talents in University (No. NCET-06-0120), the Beijing Nova of Science and Technology, Beijing Key Subject (No. XK100220555).

References

- Avnir D, Farin D, Pfeifer P, 1983. Chemistry in noninteger dimensions between two and three II: Fractal surfaces of adsorbents. *Journal of Chemical Physics*, 79: 3566–3571.
- Avnir D, Farin D, Pfeifer P, 1985. Surface geometric irregularity of particulate materials: the fractal approach. *Journal of Colloid and Interface Science*, 103: 112–123.
- Douglas J F, 1989. How does surface roughness affect polymer-surface interactions. *Macromolecules*, 22: 3707–3716.
- Edzwald J K, 1993. Coagulation in drinking water treatment: Particles, organics and coagulants. *Water Science and Technology*, 27(11): 21–35.
- Edzwald J K, Tobiasson J E, 1999. Enhanced coagulation: US requirements and a broader view. *Water Science and Technology*, 40(9): 63–70.
- El Shafei G M S, Philip C A, Moussa N A, 2004. Fractal

- analysis of hydroxyapatite from nitrogen isotherms. *Journal of Colloid and Interface Science*, 277: 410–416.
- Feder J, 1988. *Fractals*. New York: Plenum Press.
- Fripiat J J, Gatineau L, Van Damme H, 1986. Multilayer physical adsorption on fractal surfaces. *Langmuir*, 2: 562–567
- Gregory J, 1997. The density of particle aggregates. *Water Science and Technology*, 36(4): 1–13.
- Jacangelo J G, DeMarco J, Owen D M, Randtke S J, 1995. Selected processes for removing NOM: an overview. *Journal AWWA*, 87(1): 64–77.
- Jekel M R, 1986. The stabilization of dispersed mineral particles by adsorption of humic substance. *Water Research*, 20(12): 1543–1554.
- Jiang Q, Logan B E, 1991. Fractal dimensions determined from steady – state size distribution. *Environmental Science and Technology*, 25(12): 2031–2038.
- Jin P K, Wang X C, 2001. Morphological characteristics of Al-humic floc and coagulation chemistry. *Acta Scientiae Circumstantiae*, 21(suppl): 23–29.
- Li X Y, Logan B E, 2001. Permeability of fractal aggregates. *Environmental Science and Technology*, 35(14): 3373–3380.
- Mandelbrot B B, 1982. *The Fractal Geometry of Nature*. San Francisco: Freeman.
- Nègre M, Leone P, Trichet J , Défarge D, Boero V, Gennari M, 2004. Characterization of model soil colloids by cryo-scanning electron microscopy. *Geoderma*, 121(1-2): 1–16.
- Neimark A V, Unger K K, 1993. Method of discrimination of surface fractality. *Journal of Colloid and Interface Science*, 158: 412–419.
- Pfeifer P, Obert M, 1989. Fractals: basic concepts and terminology. In: *The Fractal Approach to Heterogeneous Chemistry* (Avnir D, ed.), New York: Wiley.
- Pfeifer P, Obert M, Cole M W, 1989. Fractal BET and FHH theories of adsorption: a comparative study. In: *Proceedings of the Royal Society of London. Series A, Mathematical and Physical Sciences*. Vol. 423, No. 1864, *Fractals in the Natural Sciences* May 8, 1989. Princeton, New Jersey. 169–188.
- Russ J C, 1994. *Fractal Surfaces*. New York: Plenum Press.
- Serra T, Logan B E, 1999. Collision frequencies of fractal bacterial aggregates with small particles in a sheared fluid. *Environmental Science and Technology*, 33(13): 2247–2251.
- Sokołowska Z, Sokołowski S, 1999. Influence of humic acid on surface fractal dimension of kaolin: Analysis of mercury-porosimetry and water vapour adsorption data. *Geoderma*, 88: 233–249
- Wang Y L, Lou M, Shi B Y, Wang D S, Liu J, Liao B H, 2006a. Removing humic acid in water by the integrated process of micro-eddy flocculation (MEF)-counter current dissolved air flotation (CCDAF)-nanofiltration (NF), PFC as flocculant. *Acta Scientiae Circumstantiae*, 26(5): 791–797.
- Wang Y L, Shi B Y, Du B Y, Liu J, 2006b. Surface and pore characterization of cryofixation-vacuum-freeze-dried polyferric chloride-humic acid (PFC-HA) flocs by fractal method. *Acta Scientiae Circumstantiae*, 26(9): 1474–1483.
- Wang Y L, Du B Y, Liu J, Lu J, Shi B Y, Tang H X, 2007. Surface analysis of cryofixation-vacuum-freeze-dried polyaluminum chloride-humic acid (PACl-HA) flocs. *Journal of Colloid and Interface Science*, 316: 457–466.
- Wang X C, Tambo N, 2000. A study on the morphology and density of flocs I. The fractal structure of floc. *Acta Scientiae Circumstantiae*, 20(3): 257–262.
- Yan X S, Fan J C, 1999. *Water Supply Engineering*. Beijing: Chinese construction industry press.
- Zhao Z G, 2005. *Principals for Application of Adsorption*. Beijing: Chemical industry press.